

Density Functional Characterization of Adsorption and Decomposition of 1-Propanethiol on the Ga-Rich GaAs (001) Surface

Shaobin Tang and Zexing Cao*

Department of Chemistry and State Key Laboratory of Physical Chemistry of Solid Surfaces, College of Chemistry and Chemical Engineering, Xiamen University, Xiamen 360015, China

Received: November 27, 2008; Revised Manuscript Received: March 22, 2009

Density functional calculations have been used to investigate adsorption and decomposition of 1-propanethiol on the Ga-rich GaAs (001) surface. The dissociative adsorption of 1-propanethiol on GaAs (001) to the chemisorbed propanethiolate and hydrogen was predicted to be quite facile. Followed by the C–S bond scission of the propanethiolate species, the surface propyl species was formed with a barrier of 47.2 kcal/mol for the low-energy route. The propyl species is an important precursor to propane through the C–H bond coupling and to propene via the β -H elimination. Predicted activation free energies for the surface processes from the propyl species to propane and propene are 45.2 and 37.0 kcal/mol at 298.1 K, respectively, while the corresponding overall Gibbs free energies of reaction ΔG are -49.3 and -21.2 kcal/mol relative to free 1-propanethiol. Therefore, both reaction routes are competitive, resulting in a product mixture, although the β -H elimination from the propyl species is initially remarkably favorable dynamically. On the basis of our calculations, detailed mechanisms for adsorption and thermal decomposition of 1-propanethiol on the GaAs (001) surface were proposed, and the calculated results show good agreement with experimental observations.

1. Introduction

Gallium arsenide (GaAs) as one of the most important III–V semiconductor materials has attracted considerable attention,^{1,2} and its high electron mobility and wide band gap features make GaAs quite promising in design and production of microelectronic devices. However, adsorption of impurities such as oxygen or water on the high density defect surface of GaAs-based devices might detrimentally modify their electrical characteristics due to the unwanted surface physical and chemical processes. On the contrary, the formation of self-assembled monolayers (SAMs) of organosulfur compounds on gallium arsenide semiconductor surfaces not only may enhance the resistance of GaAs to oxidation, but also may provide functional interfaces linking semiconductor surfaces to biological materials.^{3,4}

More recently, the SAMs of 1,1-biphenyl-4-thiol (BPT)⁴ and octadecyl thiol (ODT)^{5,6} on GaAs have been widely explored. Such sulfur-based processes and wet chemical treatments including ammonium sulfide,^{7,8} thionyl chloride,^{9,10} and organothiols¹¹ can generate passivating layers on the GaAs surfaces. The SAMs of alkanethiolates are quite promising in passivation of the GaAs surface. In contrast to extensively studied SAMs of hexanethiol on Au(111) and octanethiol on Cu(111) and Au(111),¹² the adsorption of alkanethiolates on the gallium arsenide surface was less investigated. Foord et al.¹³ used high-resolution electron energy loss spectroscopy (HREELS) to investigate H₂S adsorption and thermal decomposition on GaAs, and their results reveal the temperature dependence of dissociative adsorption of H₂S. Lu et al.¹⁴ performed density functional calculations on H₂S adsorption and dissociation on the gallium-rich GaAs (001) surface, and they suggested that the sulfur insertion into the Ga–As bond is more kinetically favorable.

Although the interactions of thiols up to one or two carbons on the GaAs surface have been reported,^{2,3} the adsorption and decomposition of larger thiols with more than 3 carbon atoms on GaAs surfaces are less investigated. Donev et al.¹⁵ employed the techniques of temperature programmed desorption (TPD), X-ray photoelectron spectroscopy (XPS), and time-of-flight secondary ion mass spectrometry (TOF-SIMS) to investigate the adsorption and decomposition pathways of 1-propanethiol on the Ga-rich GaAs (001) surface. Their experiments indicate that the adsorption and dissociation of 1-propanethiol on GaAs (001) may yield propanethiolate molecules and hydrogen species at room temperature. Furthermore, they observed the formation of propyl and sulfur from the C–S bond cleavage in the adsorbed propanethiolate species, as well as the consequent reactions to form propane and propene via β -H elimination and C–H bond coupling. Possible mechanisms for these surface reactions were also proposed on the basis of TPD, XPS, and TOF-SIMS investigations.

To evaluate the reaction energetics and understand the surface processes of 1-propanethiol on the Ga-rich GaAs (001) surface in detail, extensive density functional calculations have been performed. Equilibrium geometries and relative energies of adsorbed and decomposed species and detailed molecular mechanisms for these surface reactions have been explored.

2. Computational Details

The hybrid B3LYP functional¹⁶ and the LANL2DZ basis set were used to determine equilibrium geometries of reactants, intermediates, transition states, and products in the surface reaction. The nature of optimized structures was assessed by frequency calculations, and all stable minima were verified to have no imaginary frequencies, while the transition state was confirmed to have only one imaginary frequency. For comparison, calculations with the PW91¹⁷ and PBE¹⁸ functionals in combination with the *d*-augmented basis set¹⁹ for Ga and As

* To whom correspondence should be addressed. Fax: +86-592-2183047. E-mail: zxcao@xmu.edu.cn.

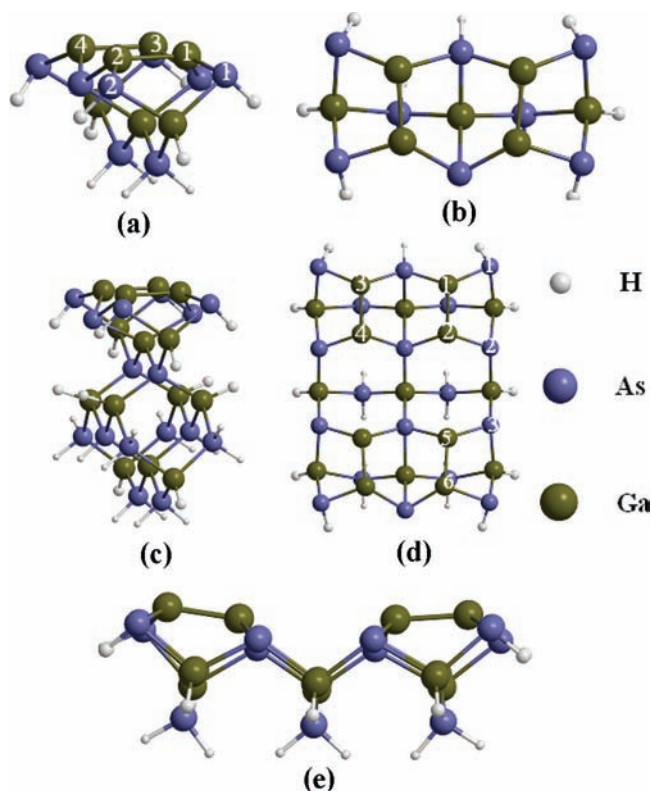


Figure 1. Optimized relaxed and dimerized Ga-rich GaAs(001) surfaces modeled by clusters $\text{Ga}_7\text{As}_8\text{H}_{11}$ (side view (a) and top view (b)), $\text{Ga}_{14}\text{As}_{16}\text{H}_{26}$ (side view (c)), and $\text{Ga}_{17}\text{As}_{18}\text{H}_{23}$ (top view (d) and side view (e)). The brown, white, and purple atoms represent Ga, H, and As atoms, respectively.

were carried out for selected species and surface processes. All calculations were performed with the Gaussian 03 program.²⁰

The gallium-rich (4×2) reconstruction on GaAs (001) was one of the most studied surface phases.^{21,22} Here we considered the clusters $\text{Ga}_7\text{As}_8\text{H}_{11}$, $\text{Ga}_{14}\text{As}_{16}\text{H}_{26}$, and $\text{Ga}_{17}\text{As}_{18}\text{H}_{23}$ representing the $\beta 2(4 \times 2)$ structure as shown in Figure 1,^{23–25} where top layers are gallium dimers tethered to “bulk” Ga atoms and “bulk” As atoms and the dangling bonds were saturated by H atoms. The number of H atoms was chosen to satisfy that the number of nonbonding electrons equals twice the number of 3-fold coordinated As atoms,^{23,26} leading to partial bulk atoms with the 3-fold or 4-fold coordination configuration. We tested other cluster models in which all dangling bonds are saturated by hydrogen atoms,²⁷ and we found that these clusters fail to reproduce the gallium-rich (001)- (4×2) reconstruction.^{23–25,28}

In the geometry optimization of these clusters, various initial structures and constraints were considered to validate a choice of computational model. For the $\text{Ga}_7\text{As}_8\text{H}_{11}$ cluster, three optimization strategies were implemented: dimerization of the top layer and fixing other layers; without dimerization of the top layer; and dimerization of the top layer and relaxing other layers. Corresponding optimized structures were denoted as Dimerized, Ideal, and Relaxed and Dimerized structures, respectively. For the $\text{Ga}_{14}\text{As}_{16}\text{H}_{26}$ and $\text{Ga}_{17}\text{As}_{18}\text{H}_{23}$ clusters, only Relaxed and Dimerized structures were optimized here.

The average binding energies per atom were defined as²⁹

$$E_b = [xE(\text{Ga}) + yE(\text{As}) + zE(\text{H}) - E(\text{Ga}_x\text{As}_y\text{H}_z)]/(x + y + z) \quad (1)$$

Table 1 presents total energies, binding energies, and selected distances of these model clusters. As Table 1 shows, predicted

binding energies and Ga–Ga separations are almost the same for three clusters with the Relaxed and Dimerized structure. The average binding energies for the Relaxed and Dimerized structure are in the range of 2.67–2.71 eV per atom, larger than the 2.44 eV for the Ideal or 2.51 eV for the Dimerized structure. Therefore, the dimerization on the top layer and relaxation of cluster may stabilize the cluster model with the GaAs (001) surface and such geometrical changes should be involved in the surface reconstruction. The surface Ga–Ga bond lengths are in the range of 2.54–2.57 Å for these Relaxed and Dimerized structures, and they are in agreement with the previous predicted value of 2.60 Å,²⁶ suggesting that the top-layer reconstruction is less dependent on the increase of the “bulk” layers and cluster sizes.

3. Results and Discussion

3.1. Adsorption and Dissociation of Propanethiol on the GaAs(001) Surface. The calculated results show that the adsorption of 1-propanethiol on $\text{Ga}_7\text{As}_8\text{H}_{11}$ is exothermic by 12.5 kcal/mol, compared to 10.8 kcal/mol (0.47 eV) for propanethiol adsorbed on the As-rich $\beta 2(2 \times 4)$ surface,³⁰ showing a notable character of chemisorption. In the complex ($\text{Ga}_7\text{C}_3\text{H}_7\text{SH}$) of $\text{C}_3\text{H}_7\text{SH}$ with the model cluster, the Ga–S dative bond has a bond length of 2.68 Å, longer than the normal Ga–S bond as shown in Figure 2. We considered other initial models of 1-propanethiol loosely associated with the cluster surface, and various starting configurations are converged to the optimized structure as shown in Figure 2a. This can be ascribed to the strong chemisorption with the Ga–S bond formation.

The H–S bond dissociation of the adsorbed 1-propanethiol leads to a chemisorbed propanethiolate ($\text{Ga}_7\text{C}_3\text{H}_7\text{S}$), where the dissociative H is transferred to the As(1). The formation of the As–H bond was confirmed to be favorable energetically in previous calculations on dissociation of H_2S on the GaAs(001)- 4×2 surface.¹⁴ As Figure 2 and Table 2 show, the dissociative adsorbed state ($\text{Ga}_7\text{C}_3\text{H}_7\text{S}$) is more stable than the initial adsorbed state ($\text{Ga}_7\text{C}_3\text{H}_7\text{SH}$) by 16.1 kcal/mol, where the Ga(1)–S bond length is reduced to 2.3 Å from 2.68 Å, in good agreement with recent studies.^{30,31}

The S–H bond dissociation of adsorbed 1-propanethiol on the GaAs(001) surface was predicted to have a barrier of 10.8 kcal/mol relative to the adsorbed species $\text{Ga}_7\text{C}_3\text{H}_7\text{SH}$. This is comparable with the dissociative adsorption of propanethiol to propanethiolate on the As-rich $\beta 2(2 \times 4)$ surface with the barrier of 0.5 ± 0.3 eV.³⁰ The predicted Gibbs free energies of reaction ΔG are -16.3 kcal/mol relative to free 1-propanethiol and thus this process should be facile as observed experimentally.¹⁵ Similar adsorbed dissociation behaviors were observed for other thiol molecules on the transition metal surfaces of Au(001)³² and Cu(110).³³

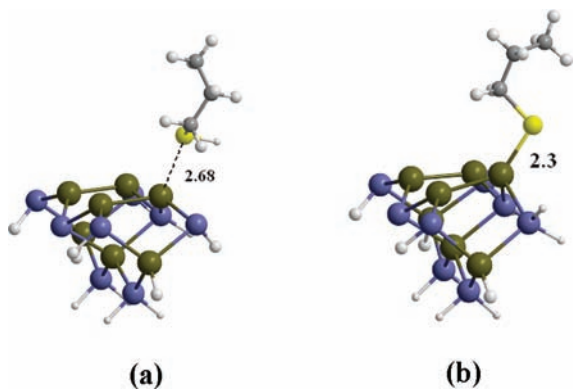
For comparison, the adsorption and dissociation of 1-propanethiol on the larger $\text{Ga}_{14}\text{As}_{16}\text{H}_{26}$ and $\text{Ga}_{17}\text{As}_{18}\text{H}_{23}$ clusters were investigated theoretically. As Tables 3 and 4 show, the optimized Ga(1)–S bond lengths and predicted barriers from the larger cluster models are almost the same as those from the relatively small cluster $\text{Ga}_7\text{As}_8\text{H}_{11}$. This provides further support to the use of the $\text{Ga}_7\text{As}_8\text{H}_{11}$ cluster in modeling the GaAs(001) surface.

The possibility of the HS– C_3H_7 bond dissociation, leading to the adsorbed SH at Ga(1) and the C_3H_7 species bonded to As(1) (see Figure 1a), was explored. Our calculations predict that the energy barrier for this process is 36 kcal/mol relative to $\text{Ga}_7\text{C}_3\text{H}_7\text{SH}$. Thus, the H– SC_3H_7 bond dissociation with a

TABLE 1: Total Energies (E_{tot} in au), Binding Energies (E_b in eV), and Selected Interatomic Distances (in Å) of Optimized Clusters $\text{Ga}_7\text{As}_8\text{H}_{11}$, $\text{Ga}_{14}\text{As}_{16}\text{H}_{26}$, and $\text{Ga}_{17}\text{As}_{18}\text{H}_{23}$ ^a

cluster	structure	E_{tot}	E_b	Ga(1)–Ga(2)	Ga(3)–Ga(4)
$\text{Ga}_7\text{As}_8\text{H}_{11}$	ideal	−69.9170	2.44 (4.23) ^b	4.0	4.0
$\text{Ga}_7\text{As}_8\text{H}_{11}$	dimerized	−69.9851	2.51 (4.35)	2.46	2.46
$\text{Ga}_7\text{As}_8\text{H}_{11}$	relaxed and dimerized	−70.1404	2.67 (4.64)	2.56	2.56
$\text{Ga}_{14}\text{As}_{16}\text{H}_{26}$	relaxed and dimerized	−142.7187	2.69 (5.04)	2.57	2.57
$\text{Ga}_{17}\text{As}_{18}\text{H}_{23}$	relaxed and dimerized	−159.4952	2.71 (4.50)	2.54	2.54

^a The atomic numberings refer to Figure 1. ^b The numbers in parentheses are defined by the following: $E_b = [xE(\text{Ga}) + yE(\text{As}) + z(\text{H}) - E(\text{Ga}_x\text{As}_y\text{H}_z)]/(x + y)$.

**Figure 2.** Optimized geometries of the adsorbed state $\text{Ga}_7\text{-C}_3\text{H}_7\text{SH}$ (a) and the dissociated adsorbed state $\text{Ga}_7\text{-C}_3\text{H}_7\text{S}$ (b). The Ga(1)–S bond length (Å) is shown, where the gray and yellow atoms represent C and S atoms, respectively.**TABLE 2: Selected Bond Lengths (in Å), Relative Enthalpies (ΔH in kcal/mol) at 0 K, and Relative Free Energies (ΔG in kcal/mol) at 298.1 K for Various Reactive States Involved in Adsorption and Decomposition of 1-Propanethiol on $\text{Ga}_7\text{As}_8\text{H}_{11}$**

species ^a	Ga(1)–S	Ga(2)–S	ΔG	ΔH
$\text{Ga}_7\text{As}_8\text{H}_{11} + \text{C}_3\text{H}_7\text{SH}$			0	0
$\text{Ga}_7\text{-C}_3\text{H}_7\text{SH}$	2.68	4.54	−2	−12.5
$\text{Ga}_7\text{-C}_3\text{H}_7\text{S-TS}$	2.51	4.58	9.3	−1.7
$\text{Ga}_7\text{-C}_3\text{H}_7\text{S}$	2.30	4.54	−16.3	−28.6
$\text{Ga}_7\text{-As-C}_3\text{H}_7\text{-1-TS}$	2.21	4.68	39.5	27.7
$\text{Ga}_7\text{-As-C}_3\text{H}_7\text{-1}$	2.12	4.46	−0.9	−10.8
$\text{Ga}_7\text{-As-C}_3\text{H}_7\text{-2-TS}$	2.23	3.11	11.1	−0.6
$\text{Ga}_7\text{-As-C}_3\text{H}_7\text{-2}$	2.62	2.21	−28	−38.2
$\text{Ga}_7\text{-As-C}_3\text{H}_8\text{-2-TS}$	2.42	2.27	32.5	21.5
$\text{Ga}_7\text{-As-C}_3\text{H}_8\text{-2}$	2.29	2.35	−48.7	−56.5
$\text{Ga}_7\text{-Ga-C}_3\text{H}_7\text{-TS}$	2.23	4.07	30.4	18.6
$\text{Ga}_7\text{-Ga-C}_3\text{H}_7$	2.22	2.47	−25.4	−37.1
$\text{Ga}_7\text{-Ga-C}_3\text{H}_7\text{-H-TS}$	2.22	2.48	−0.6	−13.2
$\text{Ga}_7\text{-Ga-C}_3\text{H}_7\text{-H}$	2.23	2.41	−43.8	−55.9
$\text{Ga}_7\text{-Ga-C}_3\text{H}_8\text{-TS}$	2.27	2.35	1.4	−13.2
$\text{Ga}_7\text{-Ga-C}_3\text{H}_8$	2.29	2.36	−49.3	−57

^a Refer to Figures 2–5.

barrier of 10.8 kcal/mol is remarkably favorable dynamically. Furthermore, our calculations exclude the possibility of the S–S bond coupling from two chemisorbed propanethiol molecules to form $\text{C}_3\text{H}_7\text{-S-S-C}_3\text{H}_7$ due to the steric repulsion interactions. On the contrary, this S–S bond coupling was observed in previous studies for methanethiol,³ and the C–S bond dissociation, yielding the methane molecule and sulfur adatom, is more facile than the S–H bond cleavage for the methylthiol adsorption on the GaAs(100)-(2×4) surface.³⁴

To evaluate the dependence of the predicted energetics on various functionals and basis sets, the PW91 and PBE functionals in combination with the basis set augmented with *d*-polarization functions were used in calculations. Table 5

TABLE 3: Selected Bond Lengths (in Å), Relative Enthalpies (ΔH in kcal/mol) at 0 K, and Relative Free Energies (ΔG in kcal/mol) at 298.1 K for Various Reactive States Involved in the Reaction to Propene

species	Ga(1)–S	Ga(2)–S	ΔG	ΔH
$\text{Ga}_{17}\text{As}_{18}\text{H}_{23} + \text{C}_3\text{H}_7\text{SH}$			0	0
$\text{Ga}_{17}\text{-C}_3\text{H}_7\text{SH}$	2.65	4.42	−4.4	−14.4
$\text{Ga}_{17}\text{-C}_3\text{H}_7\text{S-TS}$	2.49	4.5	7.9	−3.4
$\text{Ga}_{17}\text{-C}_3\text{H}_7\text{S}$	2.3	4.5	−20.3	−30.7
$\text{Ga}_{17}\text{-Ga-C}_3\text{H}_7$	2.19	2.5	−24.5	−40.9
$\text{Ga}_{17}\text{-Ga-C}_3\text{H}_6\text{-Ga-TS}$	2.22	2.44	9.6	−4.1
$\text{Ga}_{17}\text{-Ga-C}_3\text{H}_6\text{-Ga}$	2.22	2.45	4.1	−8.0
$\text{Ga}_{17}\text{-Ga-C}_3\text{H}_6\text{-As-TS}$	2.46	2.27	12.5	0.1
$\text{Ga}_{17}\text{-Ga-C}_3\text{H}_6\text{-As}$	2.56	2.22	−21.2	−31.8

TABLE 4: Selected Bond Lengths (in Å) and Relative Enthalpies (ΔH in kcal/mol) at 0 K for Various Reactive States Involved in Adsorption and Decomposition of 1-Propanethiol on $\text{Ga}_{14}\text{As}_{16}\text{H}_{26}$

geometric structures	Ga(1)–S	Ga(2)–S	ΔH
$\text{Ga}_{14}\text{As}_{16}\text{H}_{26} + \text{C}_3\text{H}_7\text{SH}$			0
$\text{Ga}_{14}\text{-C}_3\text{H}_7\text{SH}$	2.73	4.47	−10.1
$\text{Ga}_{14}\text{-C}_3\text{H}_7\text{S-TS}$	2.56	4.46	1
$\text{Ga}_{14}\text{-C}_3\text{H}_7\text{S}$	2.32	4.4	−25.1

presents selected optimized bond lengths and relative enthalpies for the S–H bond dissociation process of 1-propanethiol on the GaAs(001) surface modeled by the $\text{Ga}_7\text{As}_8\text{H}_{11}$ cluster. As Table 5 shows, all optimized geometries are quite similar, and the predicted barriers range from 5.7 to 10.8 kcal/mol, compared to 0.5 ± 0.3 eV for the adsorption dissociation of 1-propanethiol on the As-rich $\beta 2(2 \times 4)$ surface.³⁰ Generally, B3LYP calculations predict relatively larger barriers and more remarkable exothermicities than PW91 and PBE functionals. We note that these results in Table 5 are less dependent on the use of the basis sets considered here.

3.2. Decomposition of Chemisorbed Propanethiolate into Propane. Plausible mechanisms for decomposition of the surface propanethiolate species into propene or propane were

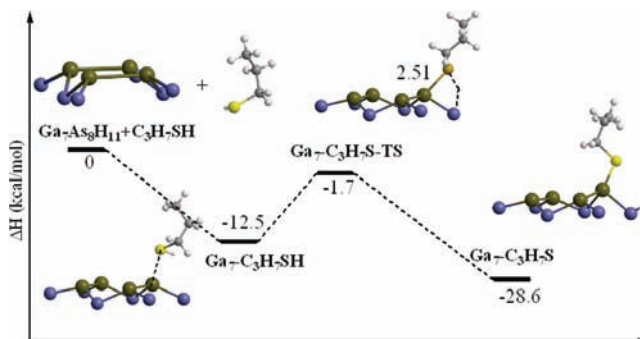
**Figure 3.** The relative energy profiles for the dissociative adsorption of 1-propanethiol on the GaAs(001) surface modeled by the $\text{Ga}_7\text{As}_8\text{H}_{11}$ cluster.

TABLE 5: Selected Optimized Bond Lengths of Ga(1)–S (*R* in Å) and Relative Enthalpies (ΔH in kcal/mol) at 0 K for the S–H Bond Dissociation of 1-Propanethiol on Ga₇As₈H₁₁ by Different Functionals and Basis Sets

species	$\Delta H/R$					
	B3LYP		PW91		PBE	
	LanL2DZ	LanL2DZ+d	LanL2DZ	LanL2DZ+d	LanL2DZ	LanL2DZ+d
Ga ₇ –C ₃ H ₇ SH	0/2.68	0/2.68	0/2.70	0/2.65	0/2.66	0/2.66
Ga ₇ –C ₃ H ₇ S–TS	10.8/2.51	10.1/2.49	6.6/2.51	5.7/2.49	6.7/2.51	5.7/2.49
Ga ₇ –C ₃ H ₇ S	–16.1/2.30	–19.0/2.28	–13.4/2.31	–15.7/2.29	–13.3/2.31	–15.3/2.29

explored in the present study. Clearly, the formation of propene or propane requires the C–S bond cleavage of the chemisorbed propanethiolate at first, leading to the surface propyl species and the chemisorbed sulfur. Followed by combination of the propyl species with the adsorbed H atom from the S–H bond activation, propane is formed. Alternatively, the β -hydrogen elimination of the propyl species yields propene. Specifically, there are two possibilities for the formation of the chemisorbed propyl, i.e., the propyl is bonded to As(2) of the second layer, or the propyl is linked to Ga(2) of the Ga-rich GaAs surface (see Figure 1 for the atomic numberings). Figures 4 and 5 and Table 2 present computational results for these surface reactions.

As Figure 4 and Table 2 show, the C–S bond cleavage of the chemisorbed propanethiolate state must overcome a barrier of 56.3 kcal/mol to form the first chemisorbed propyl state (Ga₇–As–C₃H₇–1), where the propyl is bonded to As(2) of

the second layer. This chemisorbed propyl state evolves into a more stable intermediate conformation (Ga₇–As–C₃H₇–2) through formation of a bridging S atom with a barrier of 10.2 kcal/mol and an exothermicity of 27.4 kcal/mol relative to Ga₇–As–C₃H₇–1. In Ga₇–As–C₃H₇–2, the bond lengths of Ga(1)–S and Ga(2)–S are 2.62 and 2.21 Å. The As(2)-bound propyl species couples with the adsorbed H atom from the S–H bond cleavage of the chemisorbed propanethiolate to yield propane and the model cluster with a bridging S, denoted as Ga₇–As–C₃H₈–2, where Ga(1)–S and Ga(2)–S have 2.29 and 2.35 Å bond lengths, respectively, slightly shorter than the normal Ga–S bond length of 2.37 Å.³⁵ The barrier for the C–H bond coupling is 59.7 kcal/mol. As Figure 4 and Table 2 show, the overall surface reaction to propane is exothermic by 56.5 kcal/mol, and the Gibbs free energies of reaction ΔG are –48.7 kcal/mol relative to free 1-propanethiol.

Figure 5 and Table 2 present predicted results for the formation of Ga(2)-bound propyl species. As Figure 5 shows, the C–S bond cleavage of the chemisorbed propanethiolate (Ga₇–C₃H₇S) leads to the Ga(2)-bound propyl and a bridging S on the GaAs(001) surface with a barrier of 47.2 kcal/mol and an exothermicity of 9.5 kcal/mol, denoted as Ga₇–Ga–C₃H₇. In Ga₇–Ga–C₃H₇, we note that the Ga(2)-bound propyl is far from the adsorbed H bonded to As(1) of the second layer, and thus the C–H bond coupling requires the H shift to As(2) of the second layer. As Figure 5 and Table 2 show, this H transfer process to yield an intermediate Ga₇–Ga–C₃H₇–H has a barrier of 24.9 kcal/mol and an exothermicity of 17.8 kcal/mol relative to Ga₇–Ga–C₃H₇. The C–H bond coupling in the Ga₇–Ga–C₃H₇–H state leads to propane with a barrier of 42.7 kcal/mol. The overall surface reaction to propane is exothermic by 57 kcal/mol and the corresponding Gibbs free energies of reaction ΔG are –49.3 kcal/mol. In comparison with the reaction channel shown in Figure 4, this reaction process is slightly favorable thermodynamically.

3.3. Decomposition of Chemisorbed Propanethiolate into Propene. The β -hydrogen elimination of the chemisorbed propyl species must be involved in the formation of propene, and this process requires more surface atoms. Accordingly, a relatively large Ga₁₇As₁₈H₂₃ cluster (see Figure 1d) was used to model the Ga-rich GaAs(001) surface. In the discussion of the decomposed propane pathways mentioned above, the Ga(2)-bound propyl species is relatively easily accessible with respect to the As(2)-bound propyl, and thus the Ga(2)-bound propyl served as only precursor to propene was discussed here.

Two possible initial steps for the β -H dissociative adsorption from the chemisorbed propyl were investigated in the formation of propene: (i) the β -H atom is transferred to the surface Ga(5) atom and (ii) the β -H atom is transferred to the As(2) atom of the second layer. The calculated results are shown in Figure 6 and Table 3. For the first route as shown by the black dashed lines in Figure 6, the β -H elimination of the chemisorbed propyl state has a barrier of 36.8 kcal/mol relative to Ga₁₇–Ga–C₃H₇, leading to propene and the model cluster with the adsorbed S

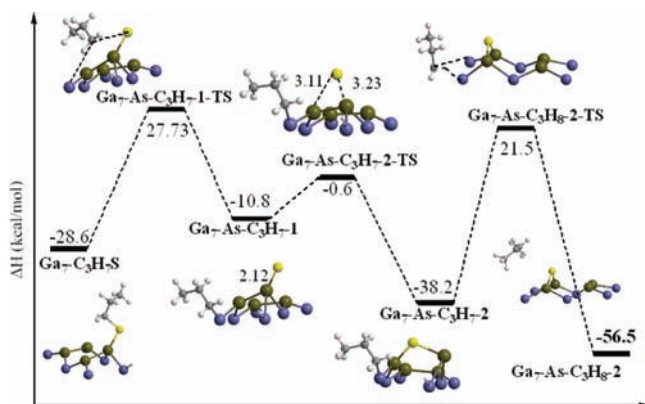


Figure 4. Relative energy profiles for the formation of propane starting from the chemisorbed propanethiolate on Ga₇–C₃H₇S. In this surface reaction pathway, the As(2) atom of the second layer is involved in the formation of the chemisorbed propyl state. The atomic numberings refer to Figure 1.

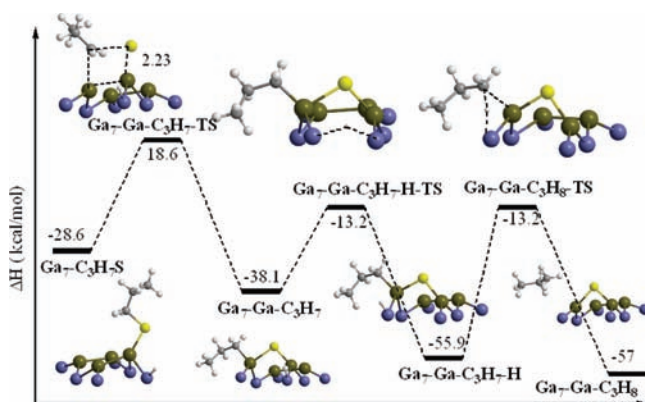


Figure 5. Relative energy profiles for the formation of propane starting from the chemisorbed propanethiolate on Ga₇–C₃H₇S. In this surface reaction pathway, the Ga(2) atom of the second layer is involved in the formation of the initial chemisorbed propyl state. The atomic numberings refer to Figure 1.

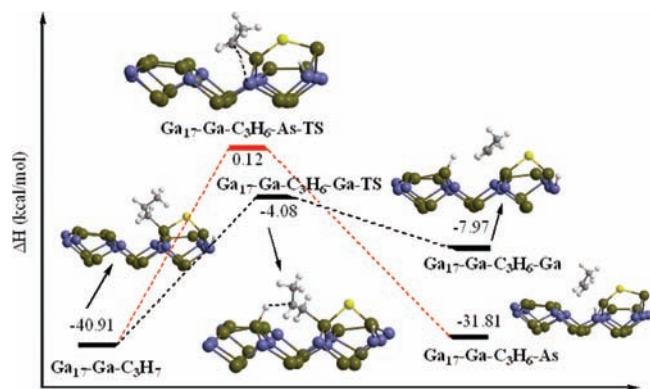


Figure 6. The relative energy profiles for the dehydrogenation of the chemisorbed propanethiolate to propene on the GaAs(001) surface modeled by the $\text{Ga}_{17}\text{As}_{18}\text{H}_{23}$ cluster. The black and red dashed lines denote the β -H transfer to the Ga(5) atom of the top layer or to the As(2) atom of the second layer, respectively. The atomic numberings refer to Figure 1.

and H atoms, denoted as $\text{Ga}_{17}\text{-Ga-C}_3\text{H}_6\text{-Ga}$. This route to propene is exothermic by 8 kcal/mol relative to free $\text{C}_3\text{H}_7\text{SH}$, while the Gibbs free energies of reaction ΔG are 4.1 kcal/mol.

For the second route involving the transfer of β -H to the As(2) atom, predicted relative energy profiles along the route to propene are displayed by the red dashed lines in Figure 6. The chemisorbed propyl ($\text{Ga}_{17}\text{-Ga-C}_3\text{H}_7$) eliminates the β -H atom to form As(2)-H and propene with a barrier of 40.9 kcal/mol. As Table 3 shows, the overall channel to propene ($\text{Ga}_{17}\text{-Ga-C}_3\text{H}_6\text{-As}$) is exothermic by 31.8 kcal/mol and the corresponding Gibbs free energies of reaction ΔG are -21.2 kcal/mol relative to free $\text{C}_3\text{H}_7\text{SH}$. Obviously, the second route to propene, where the As(2) atom of the second layer serves as the acceptor of the β -H atom, is much more favorable than the first route thermodynamically.

From Figures 4–6, we note that the sulfur atom is bridged to two Ga atoms with Ga–S bond lengths from 2.22 to 2.56 Å, after the propane or propene desorption from the surface. The presence of bridging S on the top layer will passivate the GaAs surface. Calculations indicate that the chemisorption of 1-propanethiol at the Ga(1) site on the top layer is energetically more favorable than that of other sites such as the bridge site of Ga–Ga bond and the As(1) site. A Ga←S dative bond is responsible for the strong chemisorption, where the Ga atom behaves as an acceptor and S behaves as a donor. In fact, the dissociative adsorption of 1-propanethiol, leading to the propanethiolate bonded to the surface Ga atom, also provides chemical and electronic passivation of the semiconductor surface.³⁴

3.4. Comparison of Channels to Propane and Propene.

From the calculated results in Figures 5 and 6 and Tables 2 and 3, we note that the barriers for the formation of propane and propene starting from the surface propyl species are 42.7 and 40.9 kcal/mol, respectively. Although these barrier differences are not significant, the corresponding activation free energies are 45.2 and 37.0 kcal/mol at 298.1 K for these elementary steps, respectively. This notable activation free energy difference suggests that the β -hydride elimination of the surface propyl species to propene is the major pathway, while the formation of propane via the C–H bond coupling is less favorable. This is consistent with previous experimental studies.¹⁵ Predicted relative energies for these surface processes indicate that except for 1-propanethiol that can adsorb dissociatively on the GaAs(001) surface at room temperatures, other

reaction steps involved in the channels to propane and propene need to be thermally driven as observed experimentally.¹⁵

The relative enthalpies ΔH at 0 K and relative free energies ΔG at 298.1 K for various reactive states are compiled into Tables 2 and 3. As Tables 2 and 3 show, the remarkable discrepancies between the relative enthalpies and free energies can be found for the initial adsorption step of 1-propanethiol on the GaAs(001) surface, and this arises from the entropy contribution of 1-propanethiol from the gas phase to the adsorbed state. For subsequent surface processes, the entropy effect is less important and predicted relative enthalpies and free energies are comparable. For example, the predicted activation free energies and activation enthalpies for the S–H dissociation on the GaAs(001) surface are 11.3 and 10.8 kcal/mol (Table 2), respectively. Similarly, the free energies of reaction $\Delta G(298.1\text{K})$ and enthalpies of reaction $\Delta H(0\text{K})$ for this step are -14.3 and -16.1 kcal/mol, respectively.

3.5. Comparison of Theory and Experiment. We compared our computational results with experimental data¹⁵ in order to evaluate the reliability of our theoretical treatment. As discussed above, the 1-propanethiol molecule prefers to adsorb dissociatively at the Ga site of the top layer, and this agrees with the presence of Ga–S bonding confirmed by the TOF-SIMS data experimentally.¹⁵ As Table 3 shows, the chemisorption of 1-propanethiol on the Ga-rich GaAs (001) surface was predicted to be exothermic by 14.4 kcal/mol and the corresponding free energy of adsorption ΔG is -4.4 kcal/mol. The consequent S–H bond dissociation experiences a relatively low barrier of 11 kcal/mol, and this initial surface process has a free energy of reaction ΔG of -20.3 kcal/mol. These predicted thermodynamic and dynamic properties of this surface reaction are in agreement with the experimental fact that the dissociative adsorption of 1-propanethiol to form propanethiolate molecules and hydrogen species can occur on clean GaAs (001) surface at room temperature.¹⁵ As Figures 4–6 show, the subsequent surface reactions to propane and propene experience relatively high barriers and thus the formation of their corresponding product fragments requires high temperatures. Experimentally, the main TPD peaks for propane and propene were observed at 610 and 540 K, respectively.¹⁵

4. Conclusions

The adsorption and decomposition of 1-propanethiol on the Ga-rich GaAs (001) surface have been investigated theoretically. Structures and relative stabilities of the surface reactive species and the detailed routes to propane and propene have been discussed. Our calculations show that 1-propanethiol can easily adsorb dissociatively on the clean GaAs (001) surface to generate the chemisorbed propanethiolate and hydrogen with an exothermicity of 28.6 kcal/mol. The propanethiolate may evolve to the more stable surface propyl and the chemisorbed sulfur species via the C–S scission. The combination of the propyl species and adsorbed hydrogen yields propane, whereas the β -hydride elimination from the surface propyl species generates propene, and both propane and propene subsequently can desorb to form a product mixture. Predicted activation free energies indicate that the channel to propene is favorable dynamically. Presumably, other combination reactions of the surface species, including the adsorbed propyl, sulfur, hydrogen, and propanethiolate, also can be thermally driven. Present results provide a basis to understand these surface reactions.

Acknowledgment. This work was supported by the National Science Foundation of China (20673087, 20733002, 20873105) and the Ministry of Science and Technology (2004CB719902).

References and Notes

- (1) Hong, M.; Kwo, J.; Kortan, A. R.; Mannaerts, J. P.; Sergent, A. M. *Science* **1999**, 283, 1897.
- (2) Singh, N. K.; Doran, D. C. *Surf. Sci.* **1999**, 422, 50.
- (3) Camillone, N.; Khan, K. A.; Osgood, R. M. *Surf. Sci.* **2000**, 453, 83.
- (4) Shaporenko, A.; Adlkofer, K.; Johansson, L. S. O.; Tanaka, M.; Zharnikov, M. *Langmuir* **2003**, 19, 4992.
- (5) Baum, T.; Ye, S.; Uosaki, K. *Langmuir* **1999**, 15, 8577.
- (6) Adlkofer, K.; Tanaka, M.; Hillebrandt, H.; Wiegand, G.; Bolom, T.; Deutshmann, R.; Abstreiter, G. *Appl. Phys. Lett.* **2000**, 76, 3313.
- (7) Lebedev, M. V.; Aono, M. *J. Appl. Phys.* **2000**, 87, 289.
- (8) Dong, Y.; Ding, X. M.; Hou, X. Y.; Li, Y.; Li, X. B. *Appl. Phys. Lett.* **2000**, 77, 3839.
- (9) Li, Z. S.; Cai, W. Z.; Su, R. Z.; Dong, G. S.; Huang, D. M.; Ding, X. M.; Hou, X. M.; Wang, X. *Appl. Phys. Lett.* **1994**, 64, 3425.
- (10) Wang, X.; Hou, X.; Li, Z.; Chen, X. *Surf. Interface Anal.* **1996**, 24, 564.
- (11) Lunt, S. R.; Ryba, G. N.; Santangelo, P. G.; Lewis, N. S. *J. Appl. Phys.* **1991**, 70, 7449.
- (12) Kodama, C.; Hayashi, T.; Nozoye, H. *Appl. Surf. Sci.* **2001**, 169, 264.
- (13) Foord, J. S.; FitzGerald, E. T. *Surf. Sci.* **1994**, 306, 29.
- (14) Lu, H.-L.; Chen, W.; Ding, S.-J.; Xu, M.; Zhang, D. W.; Wang, L.-K. *J. Phys. Chem. B* **2006**, 110, 9529.
- (15) Donev, S.; Brack, N.; Paris, N. J.; Pigram, P. J.; Singh, N. K.; Usher, B. F. *Langmuir* **2005**, 21, 1866.
- (16) Becke, A. D. *J. Chem. Phys.* **1993**, 98, 1372.
- (17) Perdew, J. P.; Burke, K.; Wang, Y. *Phys. Rev. B* **1996**, 54, 16533.
- (18) Perdew, J. P.; Burke, K.; Ernzerhof, M. *Phys. Rev. Lett.* **1996**, 77, 3865.
- (19) Höllwarth, A.; Böhme, M.; Dapprich, S.; Ehlers, A. W.; Gobbi, A.; Jonas, V.; Köhler, K. F.; Stegmann, R.; Veldkamp, A.; Frenking, G. *Chem. Phys. Lett.* **1993**, 208, 237.
- (20) Frisch, M. J. et al. *Gaussian 03*, revision B.05; Gaussian: Pittsburgh, PA, 2003.
- (21) Xue, Q.; Hashizume, T.; Zhou, J. M.; Sakata, T.; Ohno, T.; Sakurai, T. *Phys. Rev. Lett.* **1995**, 74, 3177.
- (22) Li, L.; Han, B.; Gan, S.; Qi, H.; Hicks, R. F. *Surf. Sci.* **1998**, 398, 386.
- (23) Fu, Q.; Li, L.; Hicks, R. F. *Phys. Rev. B* **2000**, 61, 11034.
- (24) Berger, J. F.; Pomorski, K. *Phys. Rev. Lett.* **2000**, 85, 30.
- (25) Miwa, R. H.; Miotto, R.; Ferraz, A. C.; Srivastava, G. P. *Phys. Rev. B* **2003**, 67, 045325.
- (26) Fu, Q.; Li, L.; Li, C. H.; Begarney, M. J.; Law, D. C.; Hicks, R. F. *J. Phys. Chem. B* **2000**, 104, 5595.
- (27) Pashley, M. D. *Phys. Rev. B* **1989**, 40, 10481.
- (28) Jenichen, A.; Cornelia, E. *Surf. Sci.* **2007**, 601, 900.
- (29) Schailey, R.; Ray, A. K. *J. Chem. Phys.* **1999**, 111, 8628.
- (30) Voznyy, O.; Dubowski, J. J. *J. Phys. Chem. C* **2008**, 112, 3726.
- (31) Voznyy, O.; Dubowski, J. J. *J. Phys. Chem. B* **2006**, 110, 23619.
- (32) Bondzie, V.; Dixon-Warren, St. J.; Zhang, L.; Yu, Y. *Surf. Sci.* **1999**, 431, 174.
- (33) Lai, Y.-H.; Yeh, C.-T.; Cheng, S.-H.; Liao, C. P.; Hung, W.-H. *J. Phys. Chem. B* **2002**, 106, 5438.
- (34) Lebedev, M. V. *Semiconductors* **2008**, 42, 1048.
- (35) Kohler, T.; Frauenheim, T.; Hajnal, Z.; Seifert, G. *Phys. Rev. B* **2004**, 69, 193403.

JP810435C